
DimGrow: Memory-Efficient Field-level Embedding Dimension Search

Yihong Huang
Bilibili Inc.
Shanghai, China
hyh957947142@gmail.com

Chen Chu *
Bilibili Inc.
Shanghai, China
chuchen.blueblues@gmail.com

Abstract

Key feature fields need bigger embedding dimensionality, others need smaller. This demands automated dimension allocation. Existing approaches, such as pruning or Neural Architecture Search (NAS), require training a memory-intensive SuperNet that enumerates all possible dimension combinations, which is infeasible for large feature spaces. We propose DimGrow, a lightweight approach that eliminates the SuperNet requirement. Starting training model from one dimension per feature field, DimGrow can progressively expand/shrink dimensions via importance scoring. Dimensions grow only when their importance consistently exceed a threshold, ensuring memory efficiency. Experiments on three recommendation datasets verify the effectiveness of DimGrow while it reduces training memory compared to SuperNet-based methods. Our code is available at [ur1](#).

1 Introduction

In modern deep learning models (especially recommender models), categorical features are represented by embedding vectors that neural networks can effectively process [5, 10, 42]. The dimensionality of these embedding vectors directly impacts both model performance and computational efficiency. Traditionally, practitioners often use a uniform dimension across all feature fields, which can be suboptimal as different features may require varying degrees of expressiveness to capture their underlying patterns [44]. Given the impracticality of manually tuning embedding dimensions for large-scale feature spaces, automated **Embedding Dimension Search (EDS)** methods have emerged as a promising solution.

It's important to distinguish two different levels of EDS in existing literature. **(1) Feature-level EDS** methods [9, 16, 23, 45, 19, 24, 35] determine the embedding dimension for each individual feature value. While these approaches offer maximum flexibility in dimension allocation, they introduce additional complexity in embedding lookup operations since different rows or parts in the same embedding table may have different lengths. **(2) Field-level EDS** [44, 27, 25, 6, 32], where features belonging to the same field share identical embedding dimensions, allows different fields (e.g., "gender", "user_id") to have different embedding dimensions.

While feature-level methods are particularly effective for memorization-oriented features (such as "user_id") as they can capture frequency patterns and reduce embedding dimensions for long-tail features, they may not be well-suited for the more general categorical feature fields like "gender", "age", or "device_type". These two lines of research address different problems: feature-level methods focus on optimizing memory efficiency for individual feature values based on their frequencies, while field-level EDS aims to capture the inherent expressiveness requirements of different feature fields. In this paper, we focus on **Field-level EDS**.

*Corresponding author

Challenge. Existing approaches for field-level EDS can be broadly categorized into several types. Neural Architecture Search (NAS) [28] based methods treat embedding dimensions as architectural choices and optimize them using reinforcement learning [16, 23] or evolutionary algorithms [2]. Differential Architecture Search (DARTS) [22] constructs a SuperNet with multiple dimension candidates and employs weighted selection. Pruning-based approaches [6, 43, 27] start with large embedding dimensions and gradually remove less important dimensions based on certain importance metrics. However, these approaches rely on training a memory-intensive SuperNet. This requirement poses significant challenges as it needs to training embeddings of the largest candidate dimensions for all feature fields.

Solution. To address these challenges, we propose DimGrow, a novel approach based on Shuffle Gate [13]. DimGrow assigns a learnable gate to each dimension that measures the importance of dimension by evaluating the impact of shuffling itself across samples. A gate value close to 1 indicates significant impact (greater importance), while a value near 0 suggests minimal importance (less importance). Starting from a minimal one-dimensional embedding for each feature field, we dynamically grow/shrink embedding dimensions during training. The dimension allocation process is guided by the learned importance scores: when all dimensions of a feature field consistently show high importance, we expand its embedding table by generating new dimensional parameters; conversely, dimensions with consistently low importance scores are pruned.

DimGrow follows an "allocate-as-needed" paradigm, which allows for exploring a large search space while maintaining memory efficiency. After obtaining the optimal dimension allocation, we retrain the model with the discovered configuration, completely eliminating the need for a SuperNet.

Our main contributions are summarized as follows:

- We propose DimGrow, which extends the concept of Shuffle Gate from feature selection to field-level EDS. Through a progressive dimension growth strategy, our method determines optimal embedding dimensions without requiring a memory-intensive SuperNet.
- Extensive experiments demonstrate that the dimension allocation scheme searched by DimGrow achieves stable model performance (higher AUC) with fewer embedding parameters compared to existing methods.
- Due to the elimination of SuperNet training, our approach significantly reduces memory consumption during the dimension search phase.

In our understanding, DimGrow is particularly well-suited for scenarios where the goal is to achieve optimal performance with minimal parameters (or dimensions) for a given set of feature fields.

2 Related Work

2.1 Embedding Compression

To mitigate the memory and computational costs of large embedding tables, embedding compression techniques generally fall into two categories: inter-feature and intra-feature compression [40].

Inter-feature compression reduces memory by allowing multiple features to share a limited set of embeddings. Methods such as static hashing [29, 39, 34, 26, 18, 37, 7, 46] and dynamic encoding [17, 21, 3] leverage feature frequency or learned mappings, making them particularly effective for long-tail, memorization-oriented features like "user_id" or "item_id".

Intra-feature compression, on the other hand, preserves feature individuality and compresses embeddings via quantization [41, 11, 36, 33, 20], Heuristic and Statistical Method [9], Neural Architecture Search (NAS) [44, 16, 23, 45, 19], or pruning [35, 27, 25, 6, 24, 32]. These approaches naturally align with **Embedding Dimension Search (EDS)**, which aims to reduce embedding parameters while maintaining model performance. However, to the best of our knowledge, existing methods rely heavily on training SuperNets, which not only introduces significant memory overhead during the search phase but also imposes constraints on the feasible search space.

Our work focuses on Field-level EDS, a subclass of intra-feature compression that assigns a shared embedding dimension per field and adjusts dimensions across fields. Inter-feature compression and some intra-feature [41, 11, 36, 33, 20] compression methods are orthogonal to our approach and can be combined in practice for further efficiency gains.

2.2 Field-level EDS & Feature Selection

Feature selection [12], which aims to identify and remove redundant or non-predictive feature fields while maintaining model performance, has a natural connection to Field-level EDS. Field-level EDS can be viewed as a fine-grained extension of feature selection: feature selection assigns importance scores to entire feature fields while field-level EDS evaluates the importance of individual dimensions within each field’s embedding space. Conversely, many feature selection methods that learn field-level importance can be adapted to learn dimension-level importance with minimal modifications.

This connection is evident in the parallel development of similar methodologies in both areas. For instance, AutoField [31] and AutoDim [44] both leverage DARTS [22] and Gumbel-Softmax [14] for feature/dimension selection, while SSEDs [27] and SFS [30] both evaluate importance by analyzing validation gradients of inserted masks in pre-trained models. Following this line of research, we extend Shuffle Gate [13], a feature selection method with natural polarization properties, to Field-level EDS, enabling memory-efficient and interpretable dimension importance learning.

3 PRELIMINARIES

Let $\mathcal{D} = \{(\mathbf{X}^{(n)}, y^{(n)})\}_{n=1}^N$ represent a training dataset with N samples, where each input feature vector $\mathbf{X}^{(n)} = \{\mathbf{x}_1^{(n)}, \mathbf{x}_2^{(n)}, \dots, \mathbf{x}_F^{(n)}\}$ consists of F feature fields. Each field $\mathbf{x}_i^{(n)} \in \mathbb{R}^{V_i}$ is usually encoded as a high-dimensional sparse one-hot or multi-hot vector, where V_i is the vocabulary size of the i -th field.

Embedding Layer. For the i -th feature field in the n -th sample, its embedding vector $\mathbf{e}_i^{(n)} \in \mathbb{R}^{d_i}$ is derived as $\mathbf{e}_i^{(n)} = \mathbf{E}_i \mathbf{x}_i^{(n)}$, where $\mathbf{E}_i \in \mathbb{R}^{d_i \times V_i}$ is the embedding table and d_i is the embedding dimension. The model parameters include embedding tables $\mathbf{E} = \{\mathbf{E}_1, \mathbf{E}_2, \dots, \mathbf{E}_F\}$ and neural network parameters Θ after the embedding layer. The training objective is:

$$\min_{\mathbf{E}, \Theta} \frac{1}{N} \sum_{n=1}^N \mathcal{L}(y^{(n)}, f(\mathbf{X}^{(n)}; \mathbf{E}, \Theta))$$

where \mathcal{L} is the task-specific loss function.

Field-level Embedding Dimension Search. Given the F fields embedding tables $\mathbf{E} = \{\mathbf{E}_1, \mathbf{E}_2, \dots, \mathbf{E}_F\}$, the goal is to determine the optimal embedding dimensions $\{d_1^*, d_2^*, \dots, d_F^*\}$ that minimize the total embedding parameters while maintaining model performance:

$$\{d_1^*, d_2^*, \dots, d_F^*\} = \arg \min_{\{d_1, \dots, d_F\}} \sum_{i=1}^F V_i \cdot d_i \quad \text{s.t.} \quad \text{Metric}(f_{\{d_1, \dots, d_F\}}) \geq \tau \cdot \text{Metric}(f)$$

where $f_{\{d_1, \dots, d_F\}}$ represents the model with the specified dimensions, $\text{Metric}(\cdot)$ is a performance metric (e.g., AUC), and τ controls the acceptable performance degradation.

4 METHODOLOGY

4.1 Dimension Importance Scoring via Shuffle Gate

While Shuffle Gate [13] was originally proposed for feature selection, we recognize its potential as a general approach for measuring structural importance in neural networks. The core idea of shuffle-based importance assessment stems from permutation importance analysis [8, 38]: by randomly permuting certain components while keeping others unchanged, their contribution to the model’s performance can be evaluated through the impact of this perturbation.

4.1.1 Generalized Shuffle Operation

Consider any structural components $\{\mathbf{s}_i\}$ in a neural network, where each $\mathbf{s}_i \in \mathbb{R}^{B \times *}$ (B is the batch size and $*$ denotes arbitrary remaining dimensions). This could be the embedding vector \mathbf{e}_i for one feature field, a specific embedding dimension $\mathbf{e}_{i,k}$, or an intermediate layer’s output. For each component i , we define its shuffled noise:

$$\tilde{\mathbf{s}}_i = \text{stop_gradient}(\mathbf{P}_i \mathbf{s}_i)$$

Algorithm 1: Efficient Dimension-wise Shuffling

Input: $\mathbf{s} \in \mathbb{R}^{B \times D}$: Input tensor within a batch
Output: $\tilde{\mathbf{s}} \in \mathbb{R}^{B \times D}$: Shuffled tensor
 $\mathbf{s}^T \leftarrow \text{Transpose}(\mathbf{s})$; // Transpose to $D \times B$ for efficient operation
 $\mathbf{R} \leftarrow \text{Uniform}(0, 1)^{D \times B}$; // Generate random values
 $\boldsymbol{\pi} \leftarrow \text{ArgSort}(\mathbf{R}, \text{dim} = 1)$; // Sort indices along each dimension
 $\tilde{\mathbf{s}}^T \leftarrow \text{Gather}(\mathbf{s}^T, \text{dim} = 1, \text{index} = \boldsymbol{\pi})$; // Gather values using indices
 $\tilde{\mathbf{s}} \leftarrow \text{Transpose}(\tilde{\mathbf{s}}^T)$; // Transpose back to $B \times D$
return $\tilde{\mathbf{s}}$

where $\mathbf{P}_i \in \{0, 1\}^{B \times B}$ is a random permutation matrix that reorders samples within the batch. Each \mathbf{P}_i contains exactly one 1 in each row and column, ensuring each sample appears exactly once in the shuffled result while preserving the original distribution.

For each component i , a learnable gate $g_i \in (0, 1)$ is introduced to determine how much of the original input should be preserved:

$$\begin{aligned} \mathbf{s}_i^* &= g_i \cdot \mathbf{s}_i + (1 - g_i) \cdot \tilde{\mathbf{s}}_i \\ g_i &= \sigma(\tau \cdot \theta_i) \end{aligned}$$

where σ is sigmoid function, θ_i is a learnable parameter, and τ is a temperature parameter (typically set to 5). The training loss is $\mathcal{L} = \mathcal{L}_{task} + \alpha \sum_i |g_i|$, where α controls the strength of L1 penalty.

4.1.2 Application to Dimension-level Search

Given a batch of samples $\mathbf{X} \in \mathbb{R}^{B \times d}$, for the i -th feature field’s embedding table $\mathbf{E}_i \in \mathbb{R}^{V_i \times d_i}$, we perform dimension-wise shuffling on each dimension k independently:

$$\tilde{\mathbf{e}}_{i,k} = \text{stop_gradient}(\mathbf{P}_{i,k} \mathbf{e}_{i,k})$$

where $\mathbf{e}_{i,k}$ represents the k -th embedding dimension in feature field i , and $\mathbf{P}_{i,k} \in \{0, 1\}^{B \times B}$ is a random permutation matrix. For each dimension k in feature field i , we assign a learnable gate $g_{i,k}$ that determines how much the original embedding values should be preserved:

$$\mathbf{e}_{i,k}^* = g_{i,k} * \mathbf{e}_{i,k} + (1 - g_{i,k}) * \tilde{\mathbf{e}}_{i,k} \quad (1)$$

where $g_{i,k} = \sigma(\tau \cdot \theta_{i,k})$, $\theta_{i,k}$ is a learnable parameter. The model is trained to minimize:

$$\mathcal{L} = \mathcal{L}_{task} + \alpha \sum_{i=1}^F \sum_{k=1}^{d_i} |g_{i,k}| \quad (2)$$

Through this mechanism, important dimensions will maintain high gate values to preserve their original values, while less important dimensions will have gates close to zero.

Efficient Implementation. Our implementation of the shuffling operation is detailed in Algorithm 1. The time complexity is $O(DB \log B)$, which only introduces a small overhead to the training.

4.1.3 Why Shuffle Gate?

A distinctive property of Shuffle Gate is its natural polarization - gates tend to converge to values close to 1 for important structures or 0 for unimportant ones, with few gates remaining in the intermediate range, as shown in Fig. 1.

This polarization property is intrinsic to the mechanism itself and is largely unrelated with the gates’ initial values (as long as they are not exactly 0), being primarily determined by the inherent importance of structure \mathbf{s}_i to the task loss and the strength of

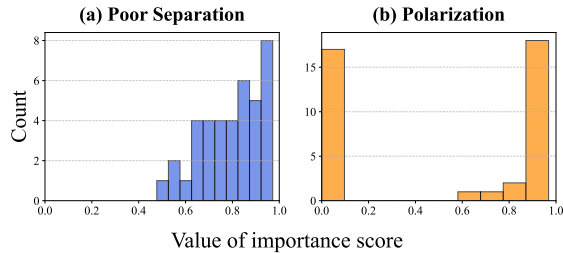


Figure 1: Shuffle Gate produces polarized importance scores with clear separation between important and unimportant components (right).

the L_1 regularization coefficient α . This behavior stands in stark contrast to mask gates, where importance scores typically fluctuate around their initial values. We give the theoretical proof in Appendix. A.1 to support this.

4.2 DimGrow: Progressive Dimension Expansion

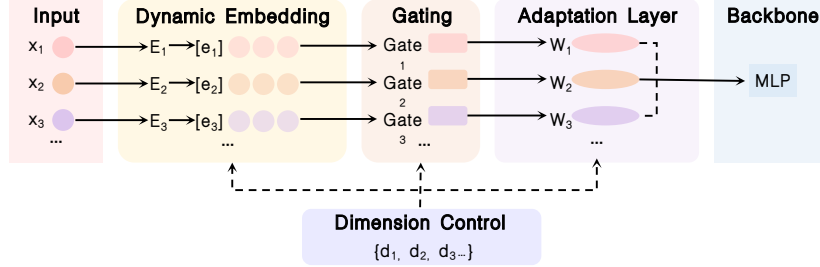


Figure 2: Framework of DimGrow

Unlike existing methods that require training a SuperNet with all possible dimension combinations, we propose a progressive dimension expansion approach that starts from minimal dimensions and dynamically grows or shrinks them based on importance scores. This design eliminates the need for maintaining a memory-intensive SuperNet while allowing for a large search space.

4.2.1 Dynamic Model Architecture

To handle dynamically updated dimensions, the model parameters consist of four main components (1) Dynamic Embedding tables \mathbf{E} , (2) Adaptation Layer W_{adapt} , (3) gating parameters θ , and (4) backbone model, as illustrated in Fig 2. In DimGrow, inputs first pass through Dynamic Embedding, then through adaptation layer for compatibility with the backbone model.

Dynamic Embedding. After the t -th gradient update step, the embedding tables are denoted as $\mathbf{E}^t = \{\mathbf{E}_1^t, \dots, \mathbf{E}_F^t\}$ where $\mathbf{E}_i^t \in \mathbb{R}^{V_i \times d_{Ai}^t}$, where d_{Ai}^t is the actual allocated dimension for table i . Let $\{d_1^t, d_2^t, \dots, d_F^t\}$ denote the *used* embedding dimensions for F feature fields, such that $d_i^t \leq d_{Ai}^t$. The embedding output for field i is:

$$\mathbf{e}_i^t = (\mathbf{E}_i^t \mathbf{x}_i)[:, : d_i^t] \in \mathbb{R}^{B \times d_i^t}$$

At initialization ($t = 0$), each feature starts with one dimension: $\mathbf{E}_i^0 \in \mathbb{R}^{1 \times V_i}$ and $d_i^0 = d_{Ai}^0 = 1$.

Adaptation Layer. Since the backbone model's input dimension remains fixed, adaptation layers are needed to transform different dimensions. Each feature field i is assigned an adapter with weight matrix $\mathbf{W}_i^t \in \mathbb{R}^{d_{Ai}^t \times d_{bb}}$ at time step t .

Each embedding output \mathbf{e}_i^t passes through a gate following Eq. (1) to produce \mathbf{e}_i^{*t} :

$$\mathbf{e}_i^{*t} = \mathbf{g}_i \odot \mathbf{e}_i^t + (1 - \mathbf{g}_i) \odot \tilde{\mathbf{e}}_i^t$$

Then, embedding features with diverse dimensions are handled by Adaptive weight:

$$\mathbf{Q}^t = \text{Concat}([\mathbf{e}_1^{*t}, \mathbf{e}_2^{*t}, \dots, \mathbf{e}_F^{*t}], \text{dim} = 1) \in \mathbb{R}^{B \times d_{\text{sum}}^t}$$

$$\mathbf{W}_{adapt}^t = \text{Concat}([\mathbf{W}_1^t[:, d_1^t], \dots, \mathbf{W}_F^t[:, d_F^t]], \text{dim} = 0) \in \mathbb{R}^{d_{\text{sum}}^t \times d_{bb}}$$

$$\mathbf{h}^t = \mathbf{Q}^t \mathbf{W}_{adapt}^t \in \mathbb{R}^{B \times d_{bb}}$$

where $d_{\text{sum}}^t = \sum_i d_i^t$. Finally, the output \mathbf{h}^t serves as the input to the backbone model:

$$\hat{y}^t = \text{bb}(\mathbf{h}^t | \Theta)$$

where $\text{bb}(\cdot | \Theta)$ represents the backbone model with parameters Θ and \hat{y}^t is the final model output.

4.2.2 Dimension Expansion and Reduction Strategy

The dimension adjustment strategy is straightforward, based on monitoring the gate values of currently used dimensions. For feature field i with used dimensions d_i^t , we examine its active gates $\{g_{i,k} | k \leq d_i^t\}$ after each update of the model parameters:

Expansion: If $\min(\{g_{i,k} | k \leq d_i^t\}) > T_{up}$, indicating all current dimensions are important, we increase d_i^t by one. When d_i^t exceeds the allocated dimension d_{Ai}^t , new parameters are generated in both \mathbf{E}_i^t and \mathbf{W}_i^t , and added to the optimizer. The expansion may also optionally be constrained by a budget on either the total dimensions (i.e., d_{sum}^t) or the total parameters (i.e., $\sum_{i=1}^F V_i \cdot d_i^t$).

To facilitate the growth of newly added dimensions, we apply a dimension-wise decaying L_1 regularization. Specifically, we modify the regularization term in Eq. (2) from $\sum_{i=1}^F \sum_{k=1}^{d_i} |g_{i,k}|$ to $\sum_{i=1}^F \sum_{k=1}^{d_i} \frac{|g_{i,k}|}{k+1}$, allowing higher dimensions to grow under weaker regularization.

Reduction: If any gate value falls below T_{down} , i.e., $\min(\{g_{i,k} | k \leq d_i^t\}) < T_{down}$, we reduce d_i^t accordingly. Note that this only decreases the used dimensions d_i^t while keeping the allocated parameters intact, allowing $0 < d_i^t \leq d_{Ai}^t$.

We initialize θ to 0, resulting in initial gate values of 0.5. Thanks to the polarization property of gates, our method is insensitive to the choice of T_{up} and T_{down} , which we set to 0.6 and 0.01 respectively. Parameter Study is presented in Sec. A.3.1. After convergence, the final dimension d_i^* for feature field i is determined by $d_i^* = |\{k | g_{i,k} > 0.5\}|$, where feature i is removed if $d_i^* = 0$. The model can then either be retrained from scratch with $\{d_i^*\}$ or fine-tuned from the current state.

5 Experiments

We conduct experiments to answer the following research questions:

RQ1: Effectiveness of Dimension Search. How does DimGrow’s dimension allocation strategy compare with existing methods?

RQ2: Search Efficiency. Without training a SuperNet, how much improvement can DimGrow achieve in terms of training speed and memory consumption during the search phase?

We have some further analysis of DimGrow in Sec. A.3.

5.1 Setup

Datasets. We evaluate our method on four public recommendation datasets: Aliccp², Avazu³, and Criteo⁴. We adopt the same data preprocessing steps as ERASE [15]. The statistics of these datasets are summarized in Table 1.

Table 1: Dataset statistics

Dataset	Avazu	Criteo	Aliccp
Data samples	40,428,967	45,850,617	85,316,519
Label Type	Click	Click	Click
Feature Num	23	39	23

Metrics. We use AUC [1] to evaluate model performance. The parameter efficiency is measured by the total number of embedding parameters: $\#params = \sum_{i=1}^F V_i \cdot d_i$, where V_i and d_i are the vocabulary size and embedding dimension of field i , respectively.

Baselines. We compare DimGrow with (1) Full Embedding Dimensions (FED) (i.e., no search), and (2) field-level EDS methods including AutoDim [44], OptEmbed-D [25], SSEDS [27], DimReg [43].

²<https://tianchi.aliyun.com/dataset/408>

³<https://www.kaggle.com/competitions/avazu-ctr-prediction>

⁴<https://ailab.criteo.com/ressources/>

For OptEmbed-D, we use its official implementations with recommended HyperParameters (HPs). For AutoDim, SSEDS, and DimReg, since no public code is available, we implement them based on their papers and tune HPs following their sensitivity studies.

Other Details. We adopt Wide&Deep [4] as the backbone model for all experiments. Initially, each feature field is allocated 16 dimensions. After obtaining the optimal dimension allocation from DimGrow and baselines, we retrain the same model for fair comparison. More details are provided in Appendix A.2.

5.2 RQ1: Effectiveness of Dimension Search

These methods can be categorized into two groups based on their compression ratio controllability. The first group, including DimGrow, DimReg, and SSEDS, allows flexible adjustment of compression ratios. The second group, consisting of OptEmbed-D and AutoDim, lacks such controllability. For fair comparison of the first group, we control the $\#params$ to be 10%, 20%, and 50% of the original $\#params$ of FED as described in Appendix. A.2.

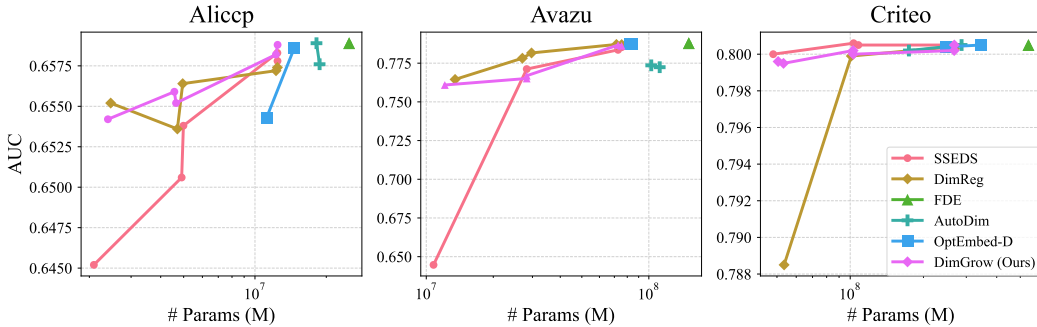


Figure 3: AUC vs. model size comparison of different embedding dimension search methods on Aliccp, Avazu, and Criteo datasets. The model size is measured in millions (M) of parameters.

As shown in Fig. 3, SSEDS exhibits notably inferior performance on Aliccp and Avazu compared to DimGrow and DimReg, particularly when the compression ratio is high (10%). Meanwhile, DimReg shows significantly worse performance on Criteo compared to DimGrow and SSEDS. In contrast, our DimGrow demonstrates stable and competitive performance across all three datasets under different compression ratios.

For OptEmbed-D and AutoDim, a notable limitation is their inability to achieve high compression ratios - they fail to compress the model below. This inflexibility in controlling model size significantly restricts their practical applications, especially in resource-constrained scenarios. Moreover, even with larger model sizes, their performance does not consistently surpass that of DimGrow, which achieves comparable or better AUC scores with much fewer parameters.

5.3 RQ2: Search Efficiency

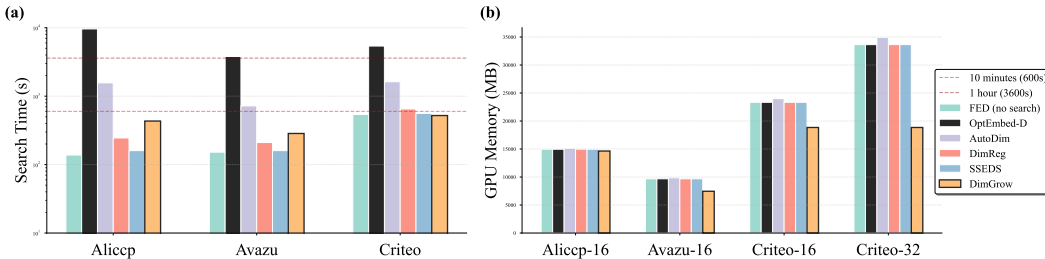


Figure 4: Computational efficiency comparison: (a) search time (in seconds) and (b) GPU memory consumption (in MB) for different embedding dimension search methods.

We measure the time consumption for generating dimension allocation schemes and GPU memory usage during the search phase. As shown in Fig. 4, we compare DimGrow with baseline methods on both search time and GPU memory consumption across different datasets.

Search Time. Since DimGrow relies on shuffle operations during training, it might introduce additional computational overhead. However, the impact varies across datasets. As illustrated in Fig. 4(a), on Aliccp and Avazu where the embedding tables are relatively small, DimGrow shows a slight increase in training time compared to FED (no search). Notably, on the Criteo dataset with larger embedding tables, DimGrow even demonstrates faster training speed than FED. .

GPU Memory Usage. The numbers after dataset names (e.g., -16, -32) indicate the field embedding dimensions. As shown in Fig. 4(b), on Aliccp-16, where embedding tables are not the memory bottleneck, all methods show similar memory consumption (around 15GB). However, the advantages of DimGrow become evident on datasets with larger embedding tables. On Avazu-16, DimGrow reduces memory usage by 23% (from 9.7GB to 7.5GB). It is also observed on Criteo-16, where DimGrow achieves a 19% reduction (from 23.3GB to 18.8GB).

Most notably, when scaling to higher dimensions on Criteo-32, SuperNet-based methods show proportional increase in memory consumption (from 23.3GB to 33.6GB), while DimGrow maintains the same memory footprint (18.8GB). This demonstrates DimGrow’s superior memory efficiency, especially when dealing with high-dimensional embedding tables.

6 Conclusion

In this paper, we propose DimGrow, a novel approach for field-level embedding dimension search that eliminates the need for training memory-intensive SuperNets. By extending the concept of Shuffle Gate from feature selection to dimension importance evaluation, DimGrow enables progressive dimension growth guided by learned importance scores. Starting from minimal dimensions, our method dynamically expands or reduces embedding dimensions based on their measured importance, achieving efficient exploration of the dimension search space while maintaining low memory overhead.

Extensive experiments on three public recommendation datasets demonstrate that DimGrow achieves competitive or superior performance compared to existing methods while significantly reducing memory consumption and search time. The effectiveness of DimGrow is particularly evident in scenarios with large embedding tables or high-dimensional embeddings, where traditional SuperNet-based approaches face significant memory constraints.

References

- [1] Andrew P Bradley. The use of the area under the roc curve in the evaluation of machine learning algorithms. *Pattern recognition*, 30(7):1145–1159, 1997.
- [2] Tong Chen, Hongzhi Yin, Yujia Zheng, Zi Huang, Yang Wang, and Meng Wang. Learning elastic embeddings for customizing on-device recommenders. In *Proceedings of the 27th ACM SIGKDD Conference on Knowledge Discovery & Data Mining*, pages 138–147, 2021.
- [3] Yizhou Chen, Guangda Huzhang, Anxiang Zeng, Qingtao Yu, Hui Sun, Heng-Yi Li, Jingyi Li, Yabo Ni, Han Yu, and Zhiming Zhou. Clustered embedding learning for recommender systems. In *Proceedings of the ACM Web Conference 2023*, pages 1074–1084, 2023.
- [4] Heng-Tze Cheng, Levent Koc, Jeremiah Harmsen, Tal Shaked, Tushar Chandra, Hrishi Aradhye, Glen Anderson, Greg Corrado, Wei Chai, Mustafa Ispir, Rohan Anil, Zakaria Haque, Lichan Hong, Vihan Jain, Xiaobing Liu, and Hemal Shah. Wide & deep learning for recommender systems. In *Proceedings of the 1st Workshop on Deep Learning for Recommender Systems, DLRS 2016*, page 7–10, New York, NY, USA, 2016. Association for Computing Machinery.
- [5] Paul Covington, Jay Adams, and Emre Sargin. Deep neural networks for youtube recommendations. In *Proceedings of the 10th ACM conference on recommender systems*, pages 191–198, 2016.
- [6] Wei Deng, Junwei Pan, Tian Zhou, Deguang Kong, Aaron Flores, and Guang Lin. Deeplight: Deep lightweight feature interactions for accelerating ctr predictions in ad serving. In *Proceedings of the 14th ACM international conference on Web search and data mining*, pages 922–930, 2021.
- [7] Aditya Desai, Li Chou, and Anshumali Shrivastava. Random offset block embedding (robe) for compressed embedding tables in deep learning recommendation systems. *Proceedings of Machine Learning and Systems*, 4:762–778, 2022.
- [8] Aaron Fisher, Cynthia Rudin, and Francesca Dominici. All models are wrong, but many are useful: Learning a variable’s importance by studying an entire class of prediction models simultaneously. *Journal of machine learning research: JMLR*, 20, 2019.
- [9] Antonio A Ginart, Maxim Naumov, Dheevatsa Mudigere, Jiyan Yang, and James Zou. Mixed dimension embeddings with application to memory-efficient recommendation systems. In *2021 IEEE International symposium on information theory (ISIT)*, pages 2786–2791. IEEE, 2021.
- [10] Carlos A Gomez-Urbe and Neil Hunt. The netflix recommender system: Algorithms, business value, and innovation. *ACM Transactions on Management Information Systems (TMIS)*, 6(4):1–19, 2015.
- [11] Hui Guan, Andrey Malevich, Jiyan Yang, Jongsoo Park, and Hector Yuen. Post-training 4-bit quantization on embedding tables. *arXiv preprint arXiv:1911.02079*, 2019.
- [12] Isabelle Guyon and André Elisseeff. An introduction to variable and feature selection. *Journal of machine learning research*, 3(Mar):1157–1182, 2003.
- [13] Yihong Huang, Chen Chu, Fan Zhang, Fei Chen, Yu Lin, Ruiduan Li, and Zhihao Li. Shufflegate: An efficient and self-polarizing feature selection method for large-scale deep models in industry, 2025.
- [14] Eric Jang, Shixiang Gu, and Ben Poole. Categorical reparameterization with gumbel-softmax, 2017.
- [15] Pengyue Jia, Yejing Wang, Zhaocheng Du, Xiangyu Zhao, Yichao Wang, Bo Chen, Wanyu Wang, Huifeng Guo, and Ruiming Tang. Erase: Benchmarking feature selection methods for deep recommender systems. In *Proceedings of the 30th ACM SIGKDD Conference on Knowledge Discovery and Data Mining*, pages 5194–5205, 2024.

- [16] Manas R Joglekar, Cong Li, Mei Chen, Taibai Xu, Xiaoming Wang, Jay K Adams, Pranav Khaitan, Jiahui Liu, and Quoc V Le. Neural input search for large scale recommendation models. In *Proceedings of the 26th ACM SIGKDD International Conference on Knowledge Discovery & Data Mining*, pages 2387–2397, 2020.
- [17] Wang-Cheng Kang, Derek Zhiyuan Cheng, Ting Chen, Xinyang Yi, Dong Lin, Lichan Hong, and Ed H Chi. Learning multi-granular quantized embeddings for large-vocab categorical features in recommender systems. In *Companion Proceedings of the Web Conference 2020*, pages 562–566, 2020.
- [18] Wang-Cheng Kang, Derek Zhiyuan Cheng, Tiansheng Yao, Xinyang Yi, Ting Chen, Lichan Hong, and Ed H Chi. Learning to embed categorical features without embedding tables for recommendation. In *Proceedings of the 27th ACM SIGKDD Conference on Knowledge Discovery & Data Mining*, pages 840–850, 2021.
- [19] Shuming Kong, Weiyu Cheng, Yanyan Shen, and Linpeng Huang. Autosrh: An embedding dimensionality search framework for tabular data prediction. *IEEE Transactions on Knowledge and Data Engineering*, 35(7):6673–6686, 2022.
- [20] Shiwei Li, Huifeng Guo, Lu Hou, Wei Zhang, Xing Tang, Ruiming Tang, Rui Zhang, and Ruixuan Li. Adaptive low-precision training for embeddings in click-through rate prediction. In *Proceedings of the AAAI Conference on Artificial Intelligence*, volume 37, pages 4435–4443, 2023.
- [21] Defu Lian, Haoyu Wang, Zheng Liu, Jianxun Lian, Enhong Chen, and Xing Xie. Lightrec: A memory and search-efficient recommender system. In *Proceedings of The Web Conference 2020*, pages 695–705, 2020.
- [22] Hanxiao Liu, Karen Simonyan, and Yiming Yang. Darts: Differentiable architecture search. *arXiv preprint arXiv:1806.09055*, 2018.
- [23] Haochen Liu, Xiangyu Zhao, Chong Wang, Xiaobing Liu, and Jiliang Tang. Automated embedding size search in deep recommender systems. In *Proceedings of the 43rd International ACM SIGIR Conference on Research and Development in Information Retrieval*, pages 2307–2316, 2020.
- [24] Siyi Liu, Chen Gao, Yihong Chen, Depeng Jin, and Yong Li. Learnable embedding sizes for recommender systems. *arXiv preprint arXiv:2101.07577*, 2021.
- [25] Fuyuan Lyu, Xing Tang, Hong Zhu, Huifeng Guo, Yingxue Zhang, Ruiming Tang, and Xue Liu. Optembed: Learning optimal embedding table for click-through rate prediction. In *Proceedings of the 31st ACM International Conference on Information & Knowledge Management*, pages 1399–1409, 2022.
- [26] Niketan Pansare, Jay Katukuri, Aditya Arora, Frank Cipollone, Riyaz Shaik, Noyan Tokgozoglul, and Chandru Venkataraman. Learning compressed embeddings for on-device inference. *Proceedings of Machine Learning and Systems*, 4:382–397, 2022.
- [27] Liang Qu, Yonghong Ye, Ningzhi Tang, Lixin Zhang, Yuhui Shi, and Hongzhi Yin. Single-shot embedding dimension search in recommender system. In *Proceedings of the 45th International ACM SIGIR conference on research and development in Information Retrieval*, pages 513–522, 2022.
- [28] Pengzhen Ren, Yun Xiao, Xiaojun Chang, Po-Yao Huang, Zhihui Li, Xiaojiang Chen, and Xin Wang. A comprehensive survey of neural architecture search: Challenges and solutions. *ACM Computing Surveys (CSUR)*, 54(4):1–34, 2021.
- [29] Hao-Jun Michael Shi, Dheevatsa Mudigere, Maxim Naumov, and Jiyan Yang. Compositional embeddings using complementary partitions for memory-efficient recommendation systems. In *Proceedings of the 26th ACM SIGKDD International Conference on Knowledge Discovery & Data Mining*, pages 165–175, 2020.

- [30] Yejing Wang, Zhaocheng Du, Xiangyu Zhao, Bo Chen, Huifeng Guo, Ruiming Tang, and Zhenhua Dong. Single-shot feature selection for multi-task recommendations. In *Proceedings of the 46th International ACM SIGIR Conference on Research and Development in Information Retrieval*, pages 341–351, 2023.
- [31] Yejing Wang, Xiangyu Zhao, Tong Xu, and Xian Wu. Autofield: Automating feature selection in deep recommender systems. In *Proceedings of the ACM Web Conference*, 2022.
- [32] Tesi Xiao, Xia Xiao, Ming Chen, and Youlong Chen. Field-wise embedding size search via structural hard auxiliary mask pruning for click-through rate prediction. *arXiv preprint arXiv:2208.08004*, 2022.
- [33] Zhiqiang Xu, Dong Li, Weijie Zhao, Xing Shen, Tianbo Huang, Xiaoyun Li, and Ping Li. Agile and accurate ctr prediction model training for massive-scale online advertising systems. In *Proceedings of the 2021 international conference on management of data*, pages 2404–2409, 2021.
- [34] Bencheng Yan, Pengjie Wang, Jinquan Liu, Wei Lin, Kuang-Chih Lee, Jian Xu, and Bo Zheng. Binary code based hash embedding for web-scale applications. In *Proceedings of the 30th ACM International Conference on Information & Knowledge Management*, pages 3563–3567, 2021.
- [35] Bencheng Yan, Pengjie Wang, Kai Zhang, Wei Lin, Kuang-Chih Lee, Jian Xu, and Bo Zheng. Learning effective and efficient embedding via an adaptively-masked twins-based layer. In *Proceedings of the 30th ACM International Conference on Information & Knowledge Management*, pages 3568–3572, 2021.
- [36] Jie Amy Yang, Jianyu Huang, Jongsoo Park, Ping Tak Peter Tang, and Andrew Tulloch. Mixed-precision embedding using a cache. *arXiv preprint arXiv:2010.11305*, 2020.
- [37] Chunxing Yin, Bilge Acun, Carole-Jean Wu, and Xing Liu. Tt-rec: Tensor train compression for deep learning recommendation models. *Proceedings of Machine Learning and Systems*, 3:448–462, 2021.
- [38] Beichuan Zhang, Chenggen Sun, Jianchao Tan, Xinjun Cai, Jun Zhao, Mengqi Miao, Kang Yin, Chengru Song, Na Mou, and Yang Song. Shark: A lightweight model compression approach for large-scale recommender systems. In *Proceedings of the 32nd ACM International Conference on Information and Knowledge Management, CIKM '23*, 2023.
- [39] Caojin Zhang, Yicun Liu, Yuanpu Xie, Sofia Ira Ktena, Alykhan Tejani, Akshay Gupta, Pranay Kumar Myana, Deepak Dilipkumar, Suvadip Paul, Ikuhiro Ihara, et al. Model size reduction using frequency based double hashing for recommender systems. In *Proceedings of the 14th ACM Conference on Recommender Systems*, pages 521–526, 2020.
- [40] Hailin Zhang, Penghao Zhao, Xupeng Miao, Yingxia Shao, Zirui Liu, Tong Yang, and Bin Cui. Experimental analysis of large-scale learnable vector storage compression. *Proc. VLDB Endow.*, 17(4):808–822, December 2023.
- [41] Jian Zhang, Jiyan Yang, and Hector Yuen. Training with low-precision embedding tables. In *Systems for Machine Learning Workshop at NeurIPS*, volume 2018, 2018.
- [42] Shuai Zhang, Lina Yao, Aixin Sun, and Yi Tay. Deep learning based recommender system: A survey and new perspectives. *ACM computing surveys (CSUR)*, 52(1):1–38, 2019.
- [43] Mingjun Zhao, Liyao Jiang, Yakun Yu, Xinmin Wang, Yi Yuan, Zheng Wei, and Di Niu. Dimreg: Embedding dimension search via regularization for recommender systems. In *Proceedings of the 2024 SIAM International Conference on Data Mining (SDM)*, pages 562–570. SIAM, 2024.
- [44] Xiangyu Zhao, Haochen Liu, Hui Liu, Jiliang Tang, Weiwei Guo, Jun Shi, Sida Wang, Huiji Gao, and Bo Long. Autodim: Field-aware embedding dimension search in recommender systems. In *Proceedings of the Web Conference 2021*, 2021.
- [45] Xiangyu Zhao, Haochen Liu, Wenqi Fan, Hui Liu, Jiliang Tang, Chong Wang, Ming Chen, Xudong Zheng, Xiaobing Liu, and Xiwang Yang. Autoemb: Automated embedding dimensionality search in streaming recommendations. In *2021 IEEE International Conference on Data Mining (ICDM)*, pages 896–905. IEEE, 2021.

- [46] Lixi Zhou, Jiaqing Chen, Amitabh Das, Hong Min, Lei Yu, Ming Zhao, and Jia Zou. Serving deep learning models with deduplication from relational databases. *arXiv preprint arXiv:2201.10442*, 2022.

NeurIPS Paper Checklist

1. Claims

Question: Do the main claims made in the abstract and introduction accurately reflect the paper's contributions and scope?

Answer: [Yes]

Justification: The abstract and introduction accurately reflect our contributions, clearly stating both the limitations of existing methods (memory overhead of SuperNet) and our solution (progressive dimension growth based on Shuffle Gate).

2. Limitations

Question: Does the paper discuss the limitations of the work performed by the authors?

Answer: [Yes]

Justification: We discuss the limitations in the Appendix, including parameter sensitivity studies and algorithmic complexity analysis.

3. Theory assumptions and proofs

Question: For each theoretical result, does the paper provide the full set of assumptions and a complete (and correct) proof?

Answer: [Yes]

Justification: We provide complete theoretical proofs in the Appendix, including the proof of dimension-level polarization property and all necessary assumptions.

4. Experimental result reproducibility

Question: Does the paper fully disclose all the information needed to reproduce the main experimental results?

Answer: [Yes]

Justification: All experimental details are described in Section 5 and Appendix, including data preprocessing, model architecture, and training parameters.

5. Open access to data and code

Question: Does the paper provide open access to the data and code?

Answer: [Yes]

Justification: All datasets used (Aliccp, Avazu, Criteo) are publicly available, and our code will be open-sourced upon paper acceptance.

6. Experimental setting/details

Question: Does the paper specify all the training and test details?

Answer: [Yes]

Justification: All experimental details are specified in Section 5 and Appendix, including dataset statistics, hyperparameter settings, and training procedures.

7. Experiment statistical significance

Question: Does the paper report error bars and statistical significance?

Answer: [Yes]

Justification: We report means and standard deviations across multiple runs and conduct statistical significance tests.

8. Experiments compute resources

Question: Does the paper provide sufficient information on the computer resources?

Answer: [Yes]

Justification: All experiments were conducted on a single NVIDIA V100 GPU, with training time and memory consumption reported in the experimental section.

9. Code of ethics

Question: Does the research conform with the NeurIPS Code of Ethics?

Answer: [Yes]

Justification: Our research fully complies with the NeurIPS Code of Ethics.

10. **Broader impacts**

Question: Does the paper discuss both potential positive and negative societal impacts?

Answer: [Yes]

Justification: Our method helps reduce computational resource consumption in recommendation systems, though it may potentially lead to reduced expressiveness for certain features.

11. **Safeguards**

Question: Does the paper describe safeguards for responsible release?

Answer: [NA]

Justification: Our method focuses on model optimization and does not involve potentially misusable pretrained models or datasets.

12. **Licenses for existing assets**

Question: Are the creators of assets properly credited and licenses respected?

Answer: [Yes]

Justification: All datasets used have clear open-source licenses and are properly cited in the paper.

13. **New assets**

Question: Are new assets well documented?

Answer: [Yes]

Justification: Our code will be open-sourced on GitHub with comprehensive documentation and usage instructions.

14. **Crowdsourcing and research with human subjects**

Question: Does the paper include details about human subject research?

Answer: [NA]

Justification: This research does not involve human subjects or crowdsourcing experiments.

15. **IRB approvals**

Question: Does the paper describe IRB approvals for human subject research?

Answer: [NA]

Justification: This research does not involve human subjects and therefore does not require IRB approval.

16. **Declaration of LLM usage**

Question: Does the paper describe the usage of LLMs?

Answer: [NA]

Justification: The core method development in this research does not involve the use of large language models.

A Technical Appendices and Supplementary Material

A.1 Theoretical Analysis of Dimension-level Polarization

Following the theoretical framework established in Shuffle Gate [13], we extend the polarization analysis to the dimension level. The key insight is that each embedding dimension can be viewed as an independent feature, allowing us to analyze its importance through the lens of shuffle-based perturbation.

Definition A.1 (ϵ -non-predictive dimension). *An embedding dimension k in feature field i is called ϵ -non-predictive with respect to a model f and loss function \mathcal{L}_{task} if the following inequality holds for all $\mathbf{x} \sim \mathcal{X}$ and for any two possible values $\mathbf{e}_{i,k}^*, \mathbf{e}_{i,k}^{j*} \in \{\mathbf{e}_{i,k}^* = g_{i,k} \mathbf{e}_{i,k} + (1 - g_{i,k}) \tilde{\mathbf{e}}_{i,k} \mid g_{i,k} \in [0, 1]\}$:*

$$|\mathcal{L}_{task}(f(\mathbf{e}_{i,k}^* | \mathbf{e}_{\setminus i,k})) - \mathcal{L}_{task}(f(\mathbf{e}_{i,k}^{j*} | \mathbf{e}_{\setminus i,k}))| \leq \epsilon \|\mathbf{e}_{i,k}^* - \mathbf{e}_{i,k}^{j*}\| \quad (3)$$

where $\mathbf{e}_{\setminus i,k}$ represents all embedding dimensions except the k -th dimension of field i .

Theorem A.2. *For an ϵ -non-predictive dimension k in feature field i , if $\alpha > \epsilon \cdot \mathbb{E}_{\mathbf{x} \sim \mathcal{X}}[\|\mathbf{e}_{i,k} - \tilde{\mathbf{e}}_{i,k}\|]$, gradient descent optimization will drive $g_{i,k}$ to 0.*

Proof. For each sample in the batch, we define:

$$\phi^{(j)}(g) = \mathcal{L}_{task}(f(g\mathbf{e}_{i,k}^{(j)} + (1-g)\tilde{\mathbf{e}}_{i,k}^{(j)} | \mathbf{e}_{\setminus i,k}^{(j)}))$$

By our condition 3, for any $g_1, g_2 \in [0, 1]$:

$$|\phi^{(j)}(g_1) - \phi^{(j)}(g_2)| \leq \epsilon \|(g_1 - g_2)(\mathbf{e}_{i,k}^{(j)} - \tilde{\mathbf{e}}_{i,k}^{(j)})\| = \epsilon |g_1 - g_2| \|\mathbf{e}_{i,k}^{(j)} - \tilde{\mathbf{e}}_{i,k}^{(j)}\|$$

Therefore, $\phi^{(j)}$ is Lipschitz continuous with constant $\epsilon \|\mathbf{e}_{i,k}^{(j)} - \tilde{\mathbf{e}}_{i,k}^{(j)}\|$. This implies:

$$|(\phi^{(j)})'(g)| \leq \epsilon \|\mathbf{e}_{i,k}^{(j)} - \tilde{\mathbf{e}}_{i,k}^{(j)}\|$$

The batch gradient becomes:

$$\left| \frac{\partial \mathcal{L}_{task}}{\partial g_{i,k}} \right| = \frac{1}{B} \sum_{\mathbf{x}^{(j)} \in \mathcal{B}} (\phi^{(j)})'(g_{i,k}) \leq \epsilon \cdot \mathbb{E}_{\mathbf{x} \sim \mathcal{X}}[\|\mathbf{e}_{i,k} - \tilde{\mathbf{e}}_{i,k}\|]$$

When $\alpha > \epsilon \cdot \mathbb{E}_{\mathbf{x} \sim \mathcal{X}}[\|\mathbf{e}_{i,k} - \tilde{\mathbf{e}}_{i,k}\|]$, we have:

$$\frac{\partial \mathcal{L}}{\partial g_{i,k}} = \frac{\partial \mathcal{L}_{task}}{\partial g_{i,k}} + \alpha > 0$$

Thus, the gradient remains positive, driving $g_{i,k}$ to 0. \square

Theorem A.3. *For a given dimension k in feature field i , if $\alpha < \mathbb{E}_{\mathbf{x} \sim \mathcal{X}}[\mathcal{L}_{task}(f(\tilde{\mathbf{e}}_{i,k} | \mathbf{e}_{\setminus i,k})) - \mathcal{L}_{task}(f(\mathbf{e}_{i,k} | \mathbf{e}_{\setminus i,k}))]$, the gate value $g_{i,k}$ will increase its value.*

Proof. For any sample $\mathbf{x}^{(j)}$ in batch \mathcal{B} , let:

$$\begin{aligned} L(\mathbf{e}_{i,k}^{(j)}) &\triangleq \mathcal{L}_{task}(f(\mathbf{e}_{i,k}^{(j)} | \mathbf{e}_{\setminus i,k}^{(j)})) \\ L(\tilde{\mathbf{e}}_{i,k}^{(j)}) &\triangleq \mathcal{L}_{task}(f(\tilde{\mathbf{e}}_{i,k}^{(j)} | \mathbf{e}_{\setminus i,k}^{(j)})) \\ L(\mathbf{e}_{i,k}^{j*}) &= L(g_{i,k} \mathbf{e}_{i,k}^{(j)} + (1 - g_{i,k}) \tilde{\mathbf{e}}_{i,k}^{(j)}) \end{aligned} \quad (4)$$

The optimization process can be approximated as the optimization of convex functions. Let $h(x)$ be convex functions. By the definition of convexity, we have:

$$h(\lambda a + (1 - \lambda)b) \leq \lambda h(a) + (1 - \lambda)h(b) \quad (5)$$

In addition, since the derivative of a convex function is monotonically increasing, we have:

$$h(x = a) \leq h(x = b) \implies h'(x)|_{x=a} \leq h'(x)|_{x=b} \quad (6)$$

By applying Eq. (5) to Eq. (4), we have:

$$L(\mathbf{e}_{i,k}^{j*}) \leq g_{i,k}L(\mathbf{e}_{i,k}^{(j)}) + (1 - g_{i,k})L(\tilde{\mathbf{e}}_{i,k}^{(j)})$$

Differentiating with respect to $g_{i,k}$:

$$\frac{\partial L(\mathbf{e}_{i,k}^{j*})}{\partial g_{i,k}} \leq L(\mathbf{e}_{i,k}^{(j)}) - L(\tilde{\mathbf{e}}_{i,k}^{(j)})$$

The total gradient including regularization is:

$$\frac{\partial \mathcal{L}}{\partial g_{i,k}} = \frac{1}{B} \sum_{\mathbf{x}^{(j)} \in \mathcal{B}} \frac{\partial L(\mathbf{e}_{i,k}^{j*})}{\partial g_{i,k}} + \alpha \leq \frac{1}{B} \sum_{\mathbf{x}^{(j)} \in \mathcal{B}} [L(\mathbf{e}_{i,k}^{(j)}) - L(\tilde{\mathbf{e}}_{i,k}^{(j)})] + \alpha$$

As batch size increases, this approaches:

$$\frac{\partial \mathcal{L}}{\partial g_{i,k}} \leq \mathbb{E}_{\mathbf{x} \sim \mathcal{X}} [L(\mathbf{e}_{i,k}) - L(\tilde{\mathbf{e}}_{i,k})] + \alpha$$

When $\alpha < \mathbb{E}_{\mathbf{x} \sim \mathcal{X}} [L(\tilde{\mathbf{e}}_{i,k}) - L(\mathbf{e}_{i,k})]$, we have:

$$\frac{\partial \mathcal{L}}{\partial g_{i,k}} < 0$$

Therefore, the negative gradient ensures that $g_{i,k}$ increases its value. □

A.2 Implementation Details of Experiments

A.3 Further Analysis

A.3.1 Parameter Sensitivity